Fluorescent and photo-oxidizing TimeSTAMP tags track protein fates in light and electron microscopy

Margaret T. Butko, Jin Yang, Yang Geng, Hyung Joon Kim, Noo Li Jeon, Xiaokun Shu, Mason R. Mackey, Mark H. Ellisman, Roger Y. Tsien, Michael Z. Lin

SUPPLEMENTARY INFORMATION

Supplementary Figure 1. An improved time-specific tag for the age measurement of proteins (TimeSTAMP2).

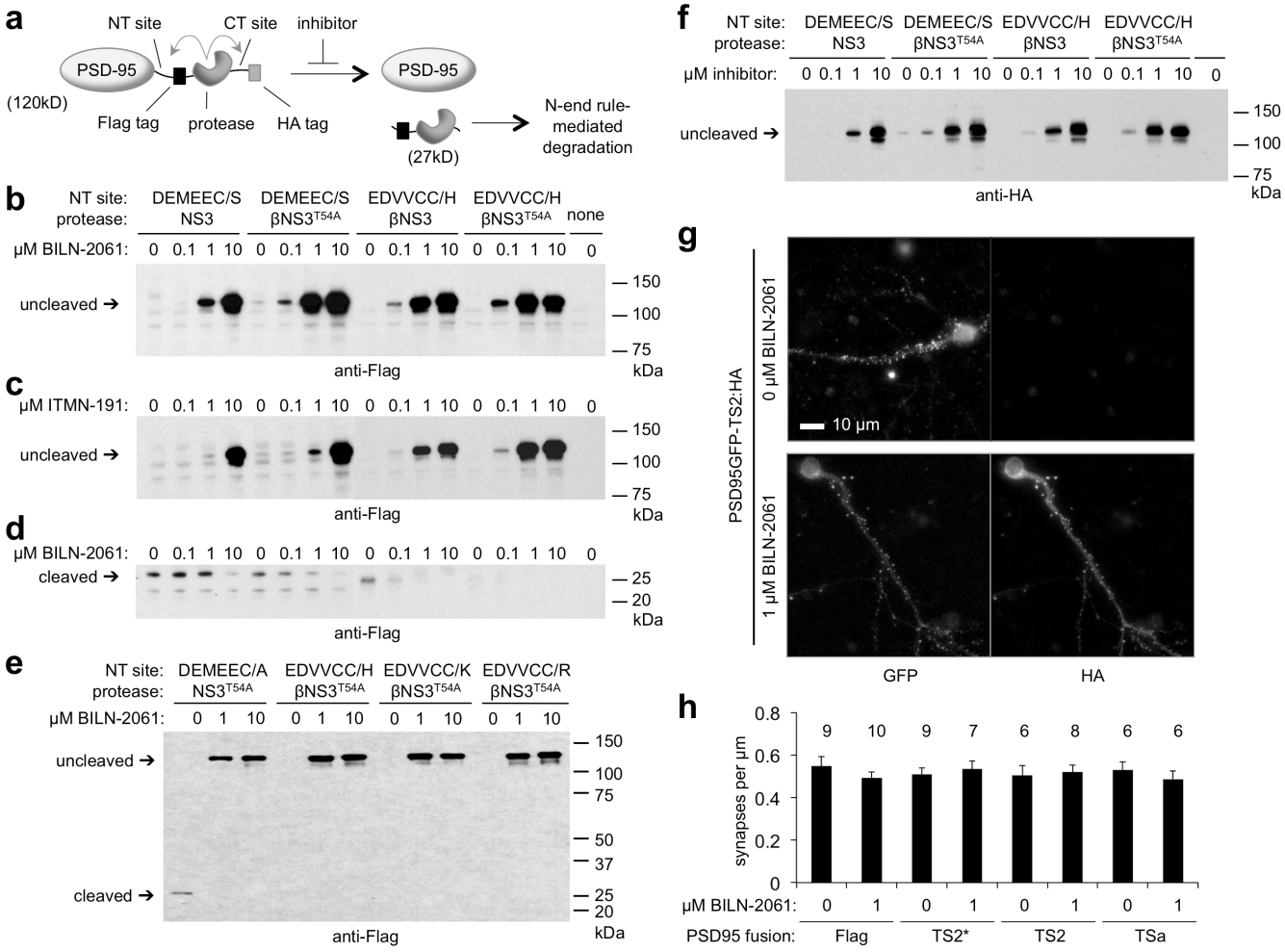

(a) General design of test constructs. HCV protease fused to PSD95 cleaves in *cis* at N-terminal (NT) and C-terminal (CT) sites, removing the HA tag. Tag removal is inhibited on proteins synthesized in the presence of inhibitor. Full-length protein should be 120 kD and tagged with both HA and Flag epitopes. Excised protease should be 27 kD and tagged with only a Flag epitope. In improved constructs, the excised protease is degraded by the N-end rule. **(b)** Immunoblots of cells expressing test constructs. Anti-Flag blotting shows that 1 μM BILN-2061 fully inhibits cleavage of the fourth construct, the TimeSTAMP2 cassette. **(c)** Similar results were obtained with a different NS3 inhibitor, ITMN-191. Lane order is the same as in **(b)**. **(d)** Anti-Flag reveals lack of accumulation of the cleaved TimeSTAMP2 cassette. Lane order is the same as in **(b)**. **(e)** Testing of various NT sites by anti-Flag blotting demonstrates that constructs with H, K, or R in the P1' position do not accumulate excised protease. **(f)** Anti-HA reveals complete block of both NT and CT cleavages in TimeSTAMP2 by 1 μM BILN-2061. **(g)** TS mediates non-toxic drug-dependent epitope tagging of PSD95 in neurons. Rat hippocampal neurons were grown for 14 days in vitro (DIV) in the absence or presence of 1 μM BILN-2061 from DIV 4 to 14. The GFP tag stably fused to PSD95 reveals protein localization independent of BILN-2061. The drug-dependent HA tag reveals PSD95 synthesized during incubation in BILN-2061. **(h)** Non-toxicity of TS2. Density of synapses was not significantly different in 14 DIV hippocampal pyramidal neurons expressing PSD95 fused to Flag or various TimeSTAMP cassettes in the absence or presence of 1 μM BILN-2061 from DIV 4 to 14. TS2* is TS2 with a protease-dead mutation (single-factor ANOVA $p=0.40$). Error bars represent standard error of the mean (SEM). The number above each bar represents the sample n for that condition.

Supplementary Figure 2. Characterization of a time-specific YFP (TS:YFP).

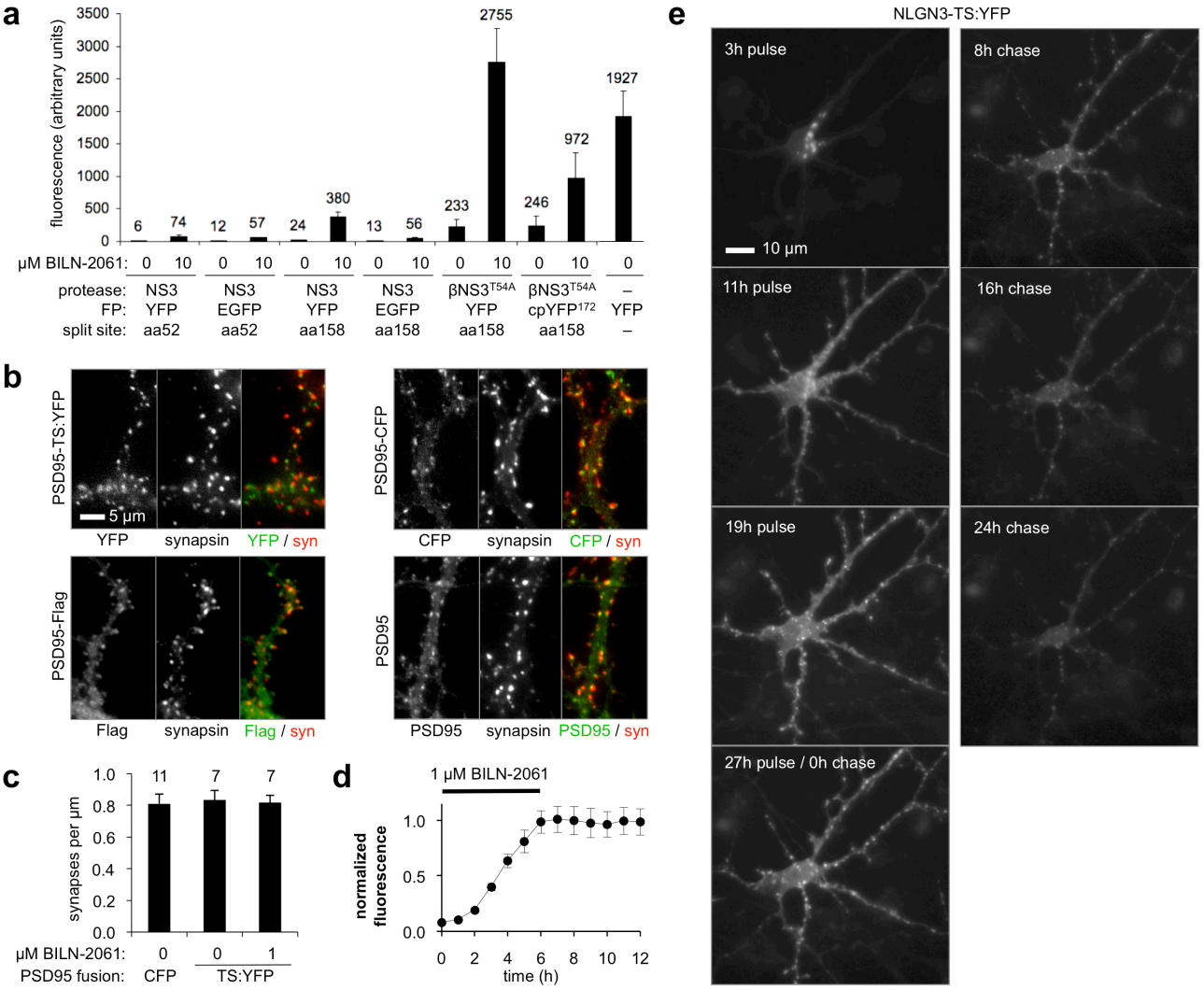

(a) Fluorescent protein domains with various TimeSTAMP cassettes insertions were tested by fusion to the C-terminus (CT) of Arc. Numbers above the bars represent mean fluorescence of 10 cells expressing cotransfected mOrange. Error bars represent SEM. Venus (YFP) with $\beta NS3^{T54A}$ inserted at amino acid 158 was designated the final TS:YFP construct. **(b)** PSD95-TS:YFP signal is localized to puncta with diameter < 0.5 µm associated with synapsin puncta, indicating synaptic localization, similar to PSD95-CFP, PSD95-Flag, or endogenous PSD95. **(c)** Synapse numbers were not significantly different in 15 DIV hippocampal pyramidal neurons expressing PSD95-CFP, or PSD95-TS:YSOG1 or PSD95-TS:YSOG2 without drug or with drug from DIV 8 to 15 (single-factor ANOVA $p = 0.964$). Numbers above the bars represent sample n. Error bars represent SEM. **(d)** Arc-TS:YFP fluorescence develops during BILN-2061 treatment and persists after drug washout. The linear accumulation of signal from 2 to 6 h is expected from new protein synthesis occurring at a constant rate within the drug application window, while extrapolation of this line down to the x-axis indicates a time delay of about 1 h due to fluorescent protein maturation. Maintenance of the induced fluorescence level after drug washout indicates irreversibility of split fluorescent protein assembly. Fluorescence in 10 random cells were normalized to peak. Error bars indicate SEM. **(e)** Live optical pulse-washout labeling with TS:YFP. Neuroligin-3 (NLGN3) was tagged at its C-terminus with TS:YFP cassette followed by duplication of the C-terminal 10 amino acids of NLGN-3 to allow for PDZ domain binding. 14-DIV neurons were imaged in the presence of 1 µM BILN-2061 to visualize accumulation of new NLGN3 (left). After drug washout, imaging was continued to follow decay of NLGN3 (right).

Supplementary Figure 3. Characterization of a time-specific orange fluorescent protein (TS:OFP).

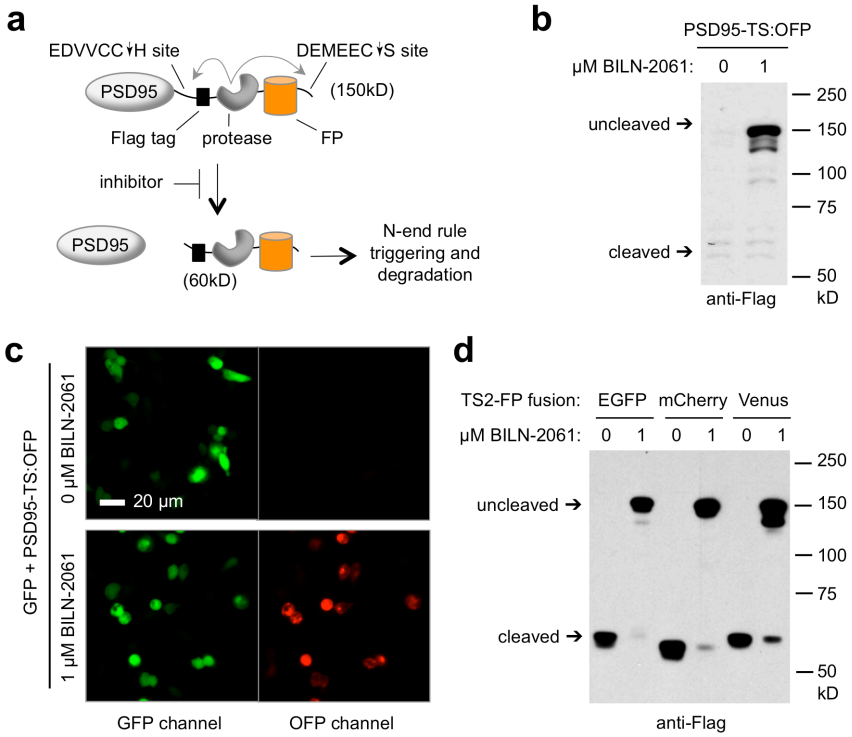

(a) Following *cis* processing of a TimeSTAMP2 cassette bearing a fluorescent protein (FP) domain fused irreversibly to the protease domain, the N-end rule should result in degradation of the protease-FP fusion. In the presence of drug, cleavage and degradation of the FP should not occur. **(b)** Immunoblots reveal N-end rule mediated degradation is efficient on a TimeSTAMP2 cassette with the mKO2 orange FP inserted C-terminal to the protease domain (TS:OFP). **(c)** Imaging shows orange fluorescent signal in HEK293 cells transfected with PSD95- TS:OFP incubated for 1 day with 1 μM BILN-2061. **(d)** EGFP, mCherry, and Venus fused to the protease domain in TimeSTAMP2 are not efficiently degraded by the N-end rule.

Supplementary Figure 4. A microfabricated chamber for localized stimulation of distal dendrites.

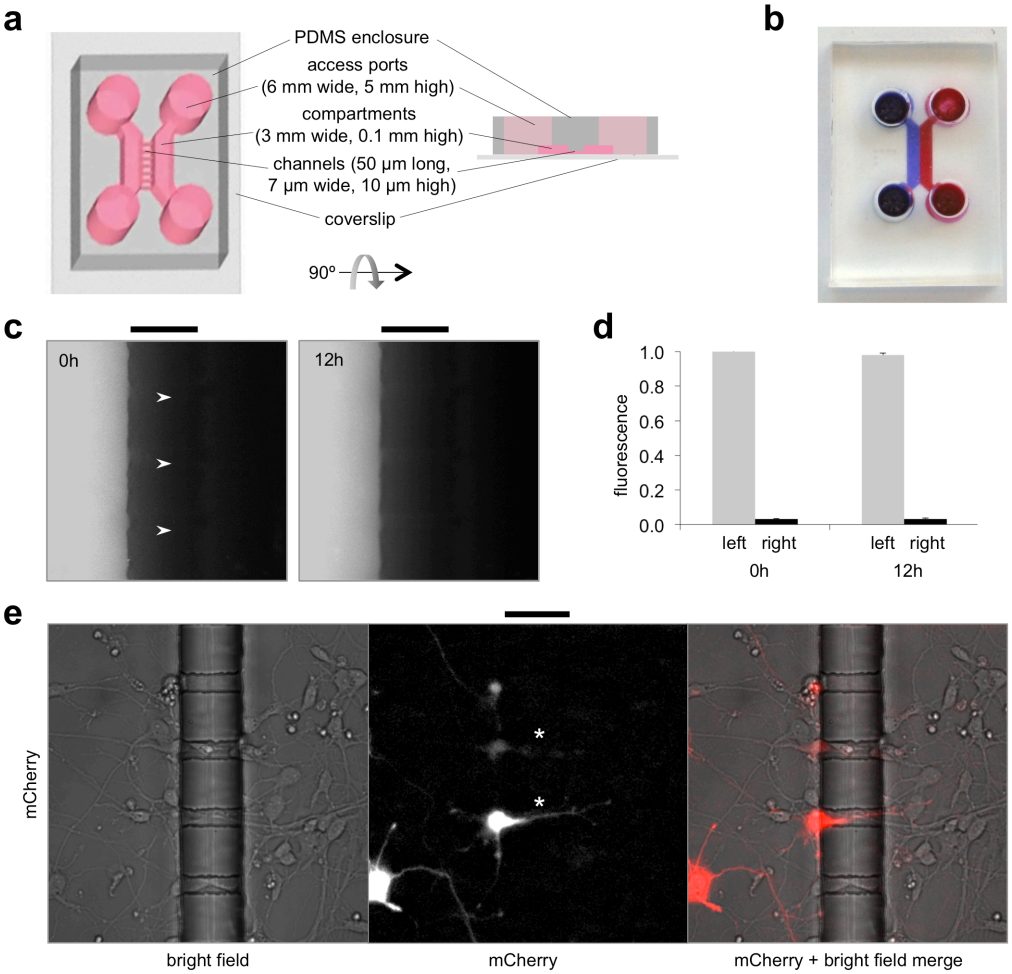

(a) Design of a compartmentalized culture chamber for performing localized stimulations on dendritic segments. Neurons with cell bodies in one compartment can extend dendrites along channels through a 50-µm barrier to the opposite compartment. **(b)** Photograph of a chamber with different color dyes placed in the two chambers to confirm fluidic separation. **(c)** Images of chambers with Alexa Fluor 647 carboxylic acid succinimidyl ester (AF647) applied to the left compartment demonstrate fluidic isolation between compartments by the 50 µm barrier (bar above images), with a steep concentration gradient within the channels (arrowheads). **(d)** Graph of integrated fluorescence intensities in the compartments at 0 and 12 h, normalized to the left compartment at time 0. Total fluorescence in the left and right compartments was measured for three fields along the center of a compartmentalized chamber. Error bars represent SEM. **(e)** Neurons extend neurites (asterisks) from one compartment to another at 5 DIV, as visualized in bright field illumination (left) and by mCherry fluorescence (center). **(c,e)** Bars above images mark the location of the 50-µm barrier, which also serves as a scale element.

Supplementary Figure 5. TS:YFP allows epitope staining of new proteins.

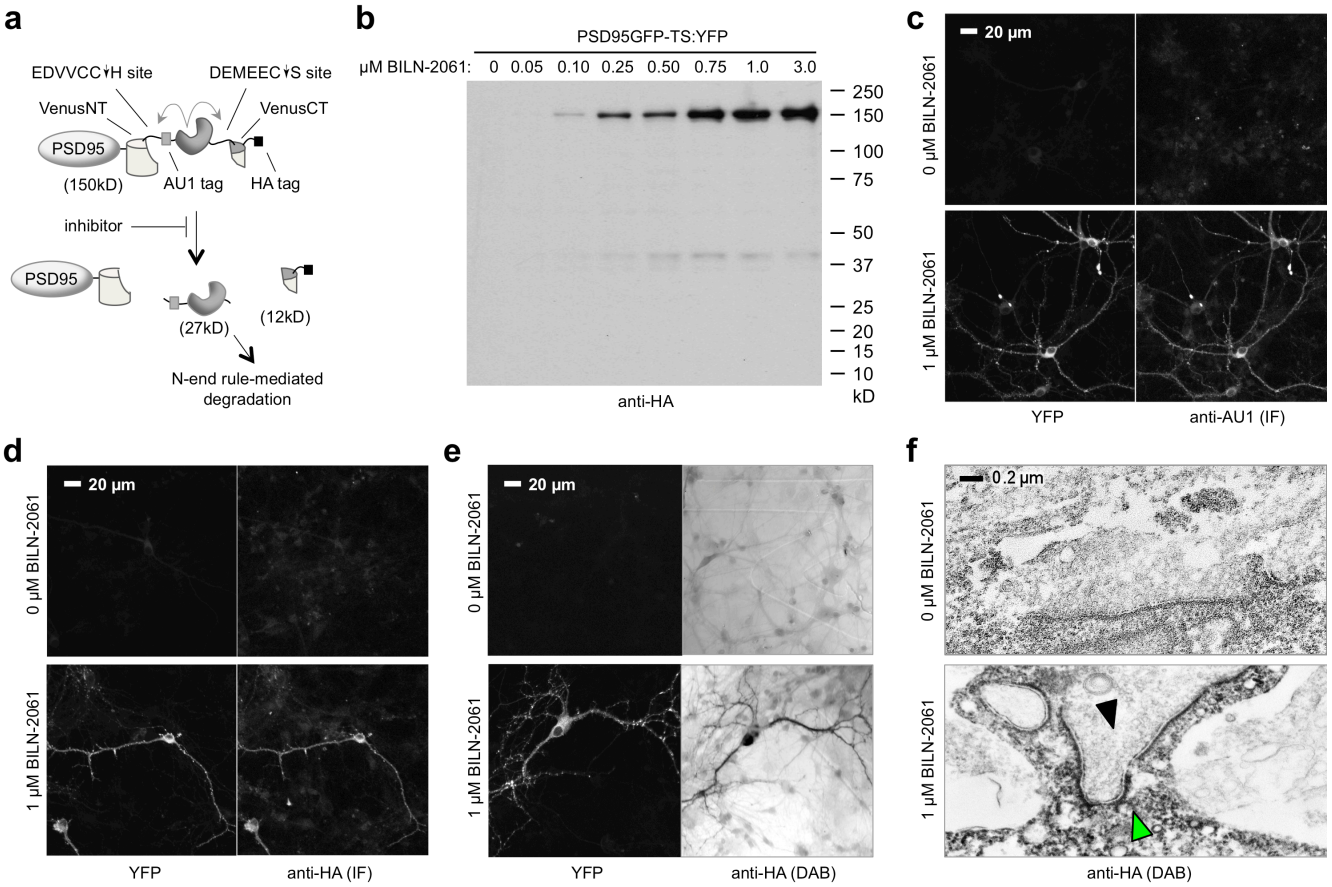

(a) In the TS:YFP cassette, an AU1 tag is located on the NS3 protease domain and an HA tag on the C-terminal YFP fragment. **(b)** Immunoblotting to an HA tag at the C-terminus of the Venus YFP demonstrates that the small YFP fragment is unstable in the absence of drug and that HA functions as a drug-dependent epitope tag with peak induction reached at 1 µM BILN-2061, similar to TS2. **(c,d)** Anti-AU1 **(c)** and anti-HA **(d)** staining correlate with YFP and is dependent on BILN-2061. **(e)** Anti-HA staining with a peroxidase-conjugated antibody mediates DAB labeling in a drug-dependent manner. **(f)** Antibody staining results in poor ultrastructural preservation in EM. Neurons expressing PSD95-TS:YFP without or with BILN-2061 were fixed, permeabilized, labelled with a peroxidase-conjugated HA antibody, and subjected to a DAB polymerization reaction. Specific signal at a membrane across from synaptic vesicles (green arrowhead) revealed successful staining of PSD95, but holes in the membrane and cytoplasm are apparent and synaptic vesicles are only partially preserved (solid arrowhead).

Supplementary Figure 6. Characterization of cleavage events in photo-oxidizing TimeSTAMP tags.

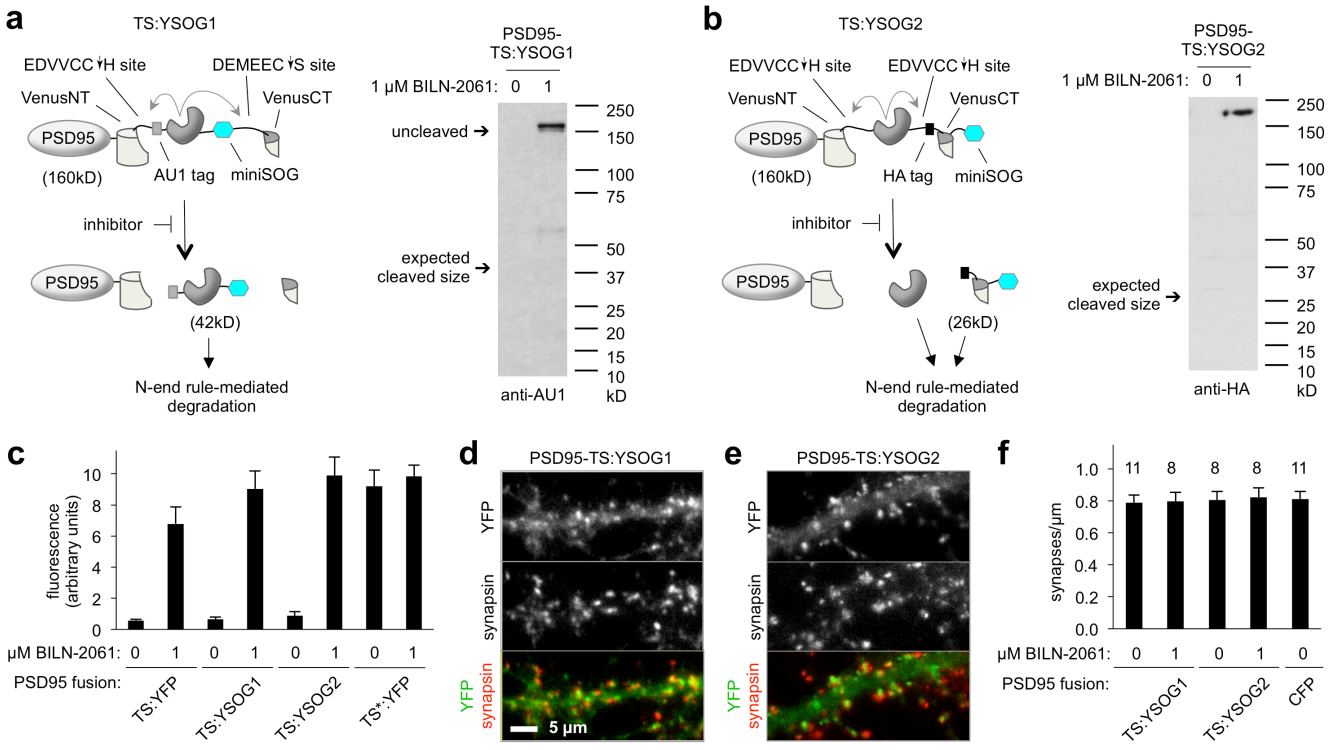

(a) An AU1 epitope tag detects the NS3-miniSOG moiety in TS:YSOG1 (left). Anti-AU1 blotting shows no accumulation of miniSOG from cleaved TS:YSOG1 in the absence of inhibitor (right). **(b)** An HA tag detects the C-terminal YFP fragment-miniSOG moiety in TS:YSOG2 (left). Anti-HA blotting shows no accumulation of miniSOG from cleaved TS:YSOG2 in the absence of inhibitor (right). **(c)** TS:YSOG1 and TS:YSOG2 exhibit similar drug-responsive fluorescence as TS:YFP. The mean background-subtracted fluorescence of 10 randomly selected HEK293 cells expressing each construct fused to PSD95 is shown for each condition. Error bars represent SEM. **(d)** Localization of PSD95-TS:YSOG1 to synaptic sites on dendritic spines by fluorescence microscopy. **(e)** Localization of PSD95-TS:YSOG2 to synaptic sites on dendritic spines by fluorescence microscopy. In **(d,e)**, fluorescence is localized to puncta with diameter < 0.5 μm associated with synapsin puncta (red), indicating synaptic localization**. (f)** Non-toxicity of photo-oxidizing TimeSTAMP tags. Density of synapses was not significantly different in 15 DIV hippocampal pyramidal neurons expressing PSD95-TS:YSOG1 or PSD95-TS:YSOG2 either without or with BILN-2061 from DIV 8 to 15, or CFP without drug (single-factor ANOVA $p = 0.997$). The number above each bar represents the sample n for that condition. Error bars represent SEM.

Supplementary Figure 7. Details of TS:YSOG1- and TS:YSOG2-mediated EM imaging.

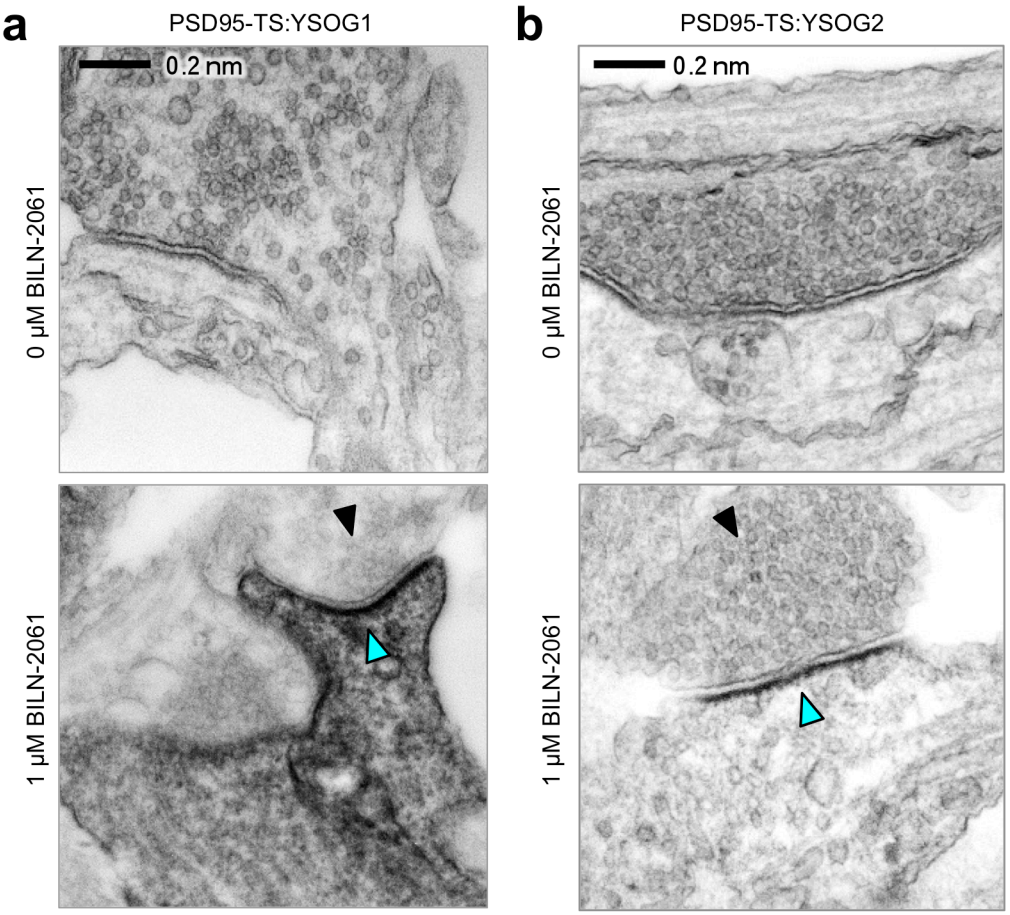

(a,b) DAB signal is specific to drug-treated samples. Neurons expressing PSD95-TS:YSOG1 **(a)** or PSD95-TS:YSOG2 **(b)** were fixed and subjected to photo-oxidation with DAB. In the absence of BILN-2061 (top), presynaptic structures are visible as accumulations of 30- to 40-nm vesicles (solid arrowhead) adjacent to a membrane with medium electron density of less then 10 nm thickness. A postsynaptic membrane is situated parallel to the presynaptic membrane separated by a constant 30-nm distance with thickness and density similar to the presynaptic membrane. In the presence of BILN-2061 (bottom), specific DAB signal appeared as intense membranous and submembranous electron densities 20–40 nm thick (cyan arrowheads) across from presynaptic structures (solid arrowheads). Compared to samples without BILN-2061, this specific DAB signal appears thicker and more intense than the electron density of the presynaptic membrane.

Supplementary Figure 8. Optimizing detection conditions for photo-oxidizing TimeSTAMP tags**.**

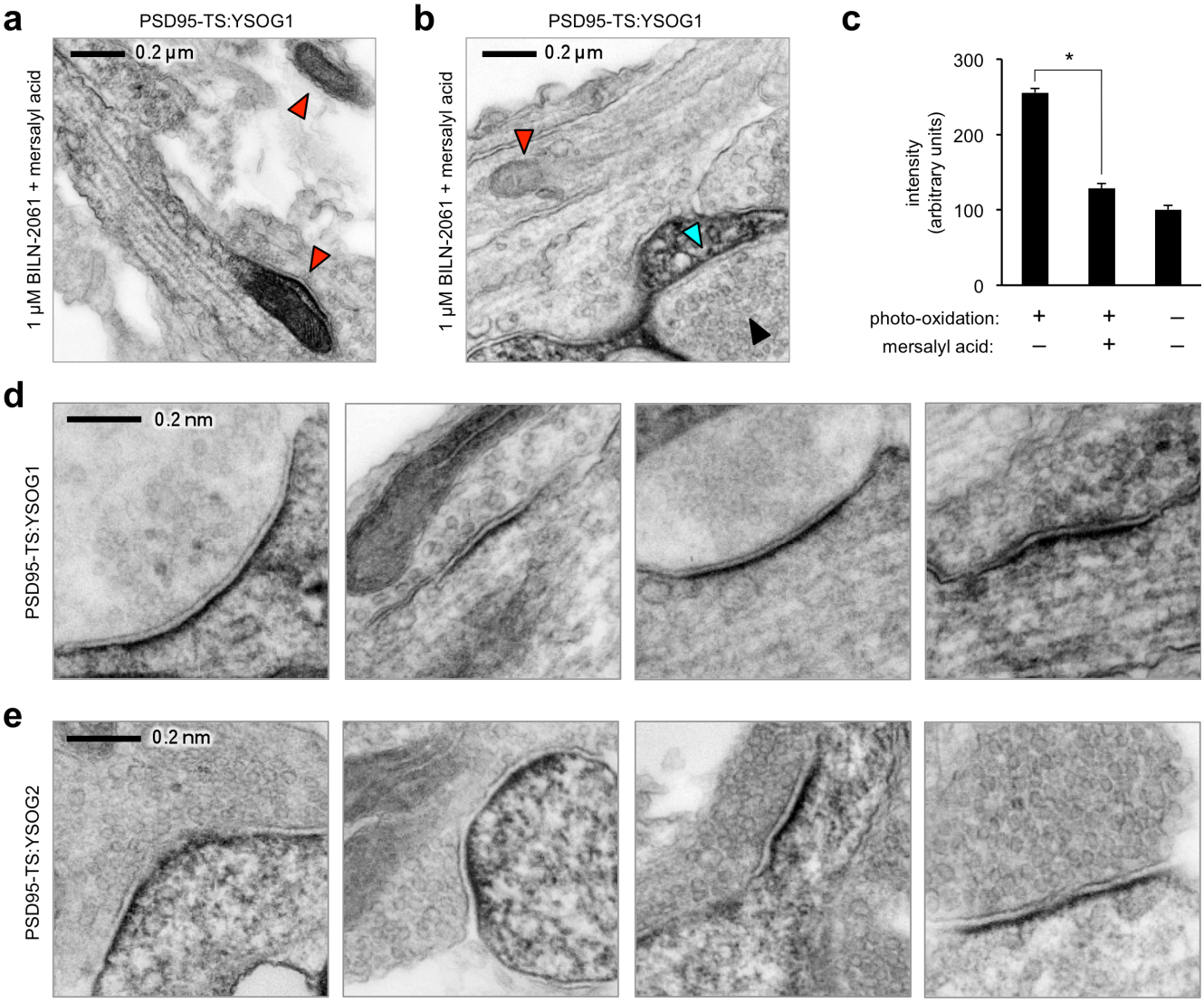

(a–c) Mersalyl acid treatment reduces mitochondrial background in photo-oxidized neurons. EM images of neurons expressing PSD95-TS:YSOG1 were photo-oxidized without **(a)** or with **(b)** mersalyl acid pretreatment. Red arrowheads indicate mitochondria. In **(b)**, DAB signal appears at a postsynaptic structure (cyan arrowhead) apposed to a presynaptic region containing abundant vesicles (solid arrowhead). **(c)** Analysis of mersalyl acid effect on mitochondrial staining. Difference between samples is statistically significant ($n = 21$ each, $p < 1 \times 10^{-6}$ by one-factor ANOVA). Mersalyl acid significantly reduced mitochondrial signal after photo-oxidation ($p < 0.0001$ by Tukey's test, asterisk), but not significantly different from no photo-oxidation ($p > 0.05$ by Tukey's test). Error bars represent SEM. **(d)** Multiple representative examples of synapses detected by TS:YSOG1. **(e)** Multiple representative examples of synapses detected by TS:YSOG2.